Journal of the Korean Ceramic Society
Vol. 53, No. 6, pp. 622~627, 2016.

http://dx.doi.org/10.4191/kcers.2016.53.6.622

Effects of Debinding Atmosphere on Properties of Sintered Reaction-bonded Si_3N_4 Prepared by Tape Casting Method

Ji-Sook Park*,, Sung-Min Lee*,‡, Yoon-Soo Han*, Hae-Jin Hwang**, and Sung-Soo Ryu*,†**

**Engineering Ceramic Center, Korea Institute of Ceramic Engineering and Technology, Icheon 17303, Korea*

***Department of Materials Science and Engineering, Inha University, Incheon 22212, Korea*

(Received September 7, 2016; Revised October 26, 2016; Accepted October 26, 2016)

ABSTRACT

The effects of the debinding atmosphere on the properties of sintered reaction-bonded Si_3N_4 (SRBSN) ceramics prepared by tape casting method were investigated. Si green tape was produced from Si slurry of Si powder, using 11.5 wt% polyvinyl butyral as the organic binder and 35 wt% dioctyl phthalate as the plasticizer. The debinding process was conducted in air and N_2 atmospheres at 400°C for 4 h. The nitridation process of the debinded Si specimens was performed at 1450°C, followed by sintering at 1850°C and 20 MPa. The results revealed that the debinding atmosphere had a significant effect on Si_3N_4 densification and thermal conductivity. Owing to the higher sintered density and larger grain size, the thermal conductivity of Si_3N_4 specimens debinded in air was higher than that of the samples debinded in N_2. Thus, debinding in air could be suitable for the manufacture of high-performance SRBSN substrates by tape casting.

Key words : Sintered reaction-bonded silicon nitride, Tape casting, Thermal property, Debinding

1. Introduction

Heat-dissipating substrates for high-power devices, which have recently gained considerable importance in the industry, require high strength, toughness, insulation, withstanding voltage, and thermal conductivity as well as low dielectric constant and pseudothermal expansion coefficient similar to those of Si chips and metal joining materials. In this context, non-oxide-based ceramics have been attracting increasing interest; in particular, Si_3N_4 has been widely studied as a suitable material, owing to its properties, which include excellent thermal-shock and chemical resistances.[1-5] Although its thermal conductivity is relatively low, compared with that of commercially AlN, Si_3N_4 can be advantageous for producing long-life and high-reliability devices, owing to its high mechanical strength and thermal-shock resistance.[6]

However, as Si_3N_4 has a high product price, its actual applications are limited.[7] To solve this issue, several studies[2,8-12] on reaction-bonded Si_3N_4 (RBSN)[13-14] have been conducted. RBSN is manufactured by using high-purity Si powder as raw material, and subjecting it to a reaction with N_2 after forming a green compact.[8-9] RBSN can greatly improve the properties of Si_3N_4 through structure densification and microstructure control; besides, its dimension can be easily controlled, owing to the low shrinkage rates and low unit costs of the manufacturing process.[15] Furthermore, the adoption of post-sintering methods allows producing materials such as sintered RBSN (SRBSN),[16,17] whose properties are similar to those of Si_3N_4 sintered by standard methods, increasing its potential commercialization.[1,2,16]

Among the different techniques for preparing green bodies, the tape casting method is widely used; it involves the preparation of a slurry by mixing ceramic powder with solvent and different organics in optimal ratios, subsequently depositing the slurry on the moving carrier film at a constant speed to form a slurry layer of uniform thickness. Preparation of uniform and highly charged green sheets is important to obtain defect-free and high-density sintered bodies by using the tape casting method.[18] Particularly, complete debinding of organic binders is essential, as residual organics act as impurities degrading the properties of the sintered body.[19]

Notably, until now, almost no reports on preparation of RBSN from Si powder by using the tape casting method have been published, although many studies on the application of tape casting to fabricate Si_3N_4 have been conducted in the past. When preparing tape cast substrates by using Si powder, oxygen impurities (such as SiO_2) present on the surfaces of the starting raw material (Si powder) may flow in during the Si slurry manufacturing, tape casting, debinding, and other processing steps.[1] As a result, the SiO_2 film formed on the Si powder surfaces obstructs the nitridation reaction to Si_3N_4, leaving residual Si, which degrades the mechanical properties of the sintered body, particularly

†Corresponding author : Sung-Soo Ryu
E-mail : ssryu@kicet.re.kr
Tel : +82-31-645-1447 Fax : +82-31-645-1485
‡Co-corresponding author: Sung-Min Lee
Email : smlee@kicet.re.kr
Tel : +82-31-645-1441, Fax : +82-31-645-1485

affecting fracture toughness and high-temperature properties; thus, the degree of nitridation should be increased by maintaining the amount of SiO_2 as low as possible.[20] In particular, thermal conductivity of Si_3N_4 substrates degrades if the organic binders are not smoothly removed during the debinding process and oxygen is solid solutioned in Si_3N_4 crystals after sintering.[21-22]

In a previous study,[23] RBSN substrates were prepared from Si powder—obtained as a byproduct of semiconductor manufacturing processes for the production of jigs or wafers—by using tape casting; the debinding process was optimized by investigating the residual carbon and oxygen contents upon variation of the debinding atmosphere and temperature, which are critical factors in the debinding process. Based on these previous results, in the present study, the effects of debinding atmosphere on nitridation, densification, and Si_3N_4 properties (such as thermal conductivity) were investigated.

2. Experimental Procedure

In this work, Si powder with average particle size of ~3 μm (Grade 4, >98.9%, VESTA Si Company, US) was ball milled at 250 rpm for 2 h in a planetary mill (Pulverisette, Fritsch, Germany) to improve its density and prepare it for the tape casting process. The scanning electron microscopy (SEM) micrographs in Fig. 1 show the morphology and particle size distribution of the ball-milled Si powder; the particle size was in the range of ~1 - 2 μm, and the average particle size was measured to be 1.24 μm.

As sintering additives, Y_2O_3 (Grade B, > 99.9%, H.C. Starck Company, Germany) and MgO (magnesium oxide, > 99.99%, Sigma-Aldrich Company, US) of ~2 μm and ~1 μm in average particle size, respectively, were used. Table 1 reports the slurry composition; the powder composition was 93 mol% Si_3N_4, 2 mol% Y_2O_3, and 5 mol% MgO.[17] For the solvent, a 50 : 50 wt% mixture of ethanol and toluene was used, along with polyvinyl butyral (BMSZ, > 97%, Sekisui chemical Co., LTD, Japan) as organic binder, dioctyl phthalate (99%, Samchun chemical, Korea) as plasticizer, and copolymer-based Disper BYK (Disper BYK®-111, Altana Company, Germany) as dispersant.

The preparation of the Si slurry for the tape casting process was conducted as follows. First, Si powder was mixed with Y_2O_3 and MgO as sintering aids in a tubular mixer (KMC-T2 3D mixer, KMC, Korea) using zirconia balls; then, after adding organics and solvent, the mixture was ball milled at 100 rpm for 24 h to obtain the final slurry.

During the tape casting process, the slurry was poured into the doctor blade of the green sheet forming machine (WNT-7002S, NTENG Co. Ltd., Korea); the film was then moved to finally obtain a 100-μm-thick green sheet. Subsequently, 1-mm-thick laminated substrates were manufactured by applying a pressure of 33 MPa for 10 s after overlapping several green sheets in a stacking machine (TMP-1000, Techgen, Korea). To increase the green sheet density, the substrates were compressed for 10 min by applying a pressure of 20 MPa at 70°C in a warm isostatic press (TWP-1000, Techgen, Korea). After compression, the substrates were cut into smaller pieces of 30 × 30 mm^2 by using a cutting machine (AMX-2100A, Automax, Korea).

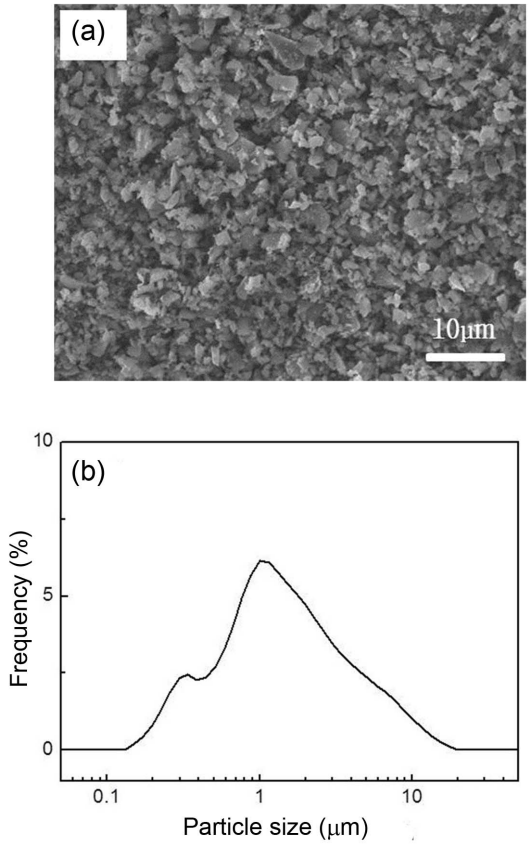

Fig. 1. (a) SEM images and (b) particle size distributions of Si powder used as a starting material.

Table 1. Formulation of Si Slurry for Tape Casting

Power (wt%)	Solvent (wt%)	Dispersant (wt%)	Binder (PVB) (wt%)	Plasticizer (DOP) (wt%)
43.21	49.69	0.39	4.97 (P/S=11.5%)	1.74

To investigate the effects of the debinding atmosphere, the laminated Si substrates were subjected to debinding in air and N_2 atmospheres. The temperature was maintained at 400°C for 4 h, with a temperature rise rate of 5°C/min. The debinding processes in air and N_2 were conducted in a box-type electric furnace and in a tube-type electric furnace (HeeWoong ENG, Korea), respectively. In the case of the N_2 atmosphere, purity of class 5N was used at the flux of 1 L/min.

For the nitriding process, temperatures were raised through several stages up to the range of ~1200 - 1450°C for 22 h, followed by furnace cooling down to room temperature, while using the a gas mixture of $95N_2$-$5H_2$ at the flux of 1 L/min.[17]

Si_3N_4 substrates were completely covered using a 50 : 50 wt% mixture of Si_3N_4 and BN powders, placed on a graphite crucible, and then sintered for 6 h in N_2 atmosphere at 20 MPa and up to 1850°C at the temperature rise rate of 10°C/min by using a hot isostatic press (AIP6-30H, AIP, US).

For the specimens subjected to the nitriding process, the nitriding ratio was determined by measuring the specimen weights before and after the nitriding reaction; the ratio of the amount of Si converted to Si_3N_4 after nitriding reaction to the initial amount of Si in the green compact specimen was obtained.[1,7] For the analysis of the α-Si_3N_4 and β-Si_3N_4 crystalline phases present in the specimens, X-ray diffraction (XRD) patterns were obtained after nitridation and sintering in the 2θ range of 20° - 40° at 40 kV and 100 mA by using an X-ray diffractometer (D/max-2500, Rigaku, Japan). To analyze the microstructures, the sintered specimens were polished and then examined by field-emission scanning electron microscopy (FE-SEM; JSM-6701F, Jeol, Japan) after the polished surface was etched by a plasma etcher. Using Archimedes' principle, the density of the Si_3N_4 sintered bodies was measured, and thermal conductivity was determined by xenon flash analysis (XFA 600, Linseis, Germany). Thermal conductivity was calculated through the following equation; to reduce measurement errors, a mean value was used after three measurements:

$$\lambda(T) = a(T) \times \rho(T) \times C_p(T) \quad (1)$$

where $a(T)$ is the thermal diffusion coefficient (mm^2/s), $\rho(T)$ is the density (g/cm^3), and $C_p(T)$ is the specific heat (J/gK).

3. Results and Discussion

The nitridation degree of the nitrided specimens was calculated after nitridation at 1450°C following debinding in air and N_2 atmospheres (Table 2). The degree of nitridation of the specimens debinded in air, 70.9%, was lower than that of the samples debinded in N_2 atmosphere, 72.6%. This result was attributed to the fact that, for the samples debinded in N_2, the amount of SiO_2 layer on the Si particle surfaces was relatively smaller than that observed for the specimens debinded in air. When the amount of SiO_2 is small, a modest quantity of liquid phase is generated, resulting in the reduction of the blocking of the pore channels and leading to a relatively high degree of nitridation.[1]

Figure 2 shows the XRD patterns for specimens subjected to nitridation in different debinding atmospheres. Notably, α-Si_3N_4 and β-Si_3N_4 phases were formed through reactions of the Si phase with N_2. Both specimens debinded in air and N_2 atmospheres showed similar patterns exhibiting α-Si_3N_4 and β-Si_3N_4 crystal phases. However, the β-Si_3N_4 peak intensity for the specimen debinded in air was higher than that observed for the sample debinded in N_2; in addition, the intensities of the peaks of the secondary phases, i.e., $Y_4Si_2O_7N_2$ and $Y_2Si_3O_3N_4$, which were formed from the reaction between SiO_2 and sintering aids, were found to be slightly higher for the air-debinded sample.

Notably, although the nitridation appeared to have been fully accomplished because of the absence of residual Si peaks in the XRD patterns, the degrees of nitridation for both specimens were low, ~70%, as shown in Table 2; this could be attributed to various factors. The first factor involved the calculation of the degree of nitridation; this was obtained by including Si for which oxidation had progressed, while the calculation of the degree of nitridation is conducted considering unoxidized Si; as a result, the calculated degree of nitridation was lower than the actual degree of nitridation. The oxygen content in the laminated substrates after debinding was 5.3% in air and 4.2% in N_2. Even when complete nitridation was assumed by calculating the content of pure unoxidized Si after excepting by 2.07% owing to the oxygen content in the sintering aid, the degree of nitridation was found to be ~ 94%.

The second factor was the amount of residual oxygen after the debinding process. According to the result of the thermogravimetric analysis on laminated substrates after debinding, an additional ~ 1% reduction of the weight occurred. The oxygen contained in the binder was considered to have decomposed during the nitridation process.

The third factor involved the reactions occurring at the

Table 2. The Degree of Nitridation (R_N) of Si_3N_4 Substrates Debinded in Air and N_2 Atmosphere after Nitriding at 1450°C

	1450°C Nitriding 400°C Air Debinding	1450°C Nitriding 400°C N_2 Debinding
R_N (%)	70.9	72.6

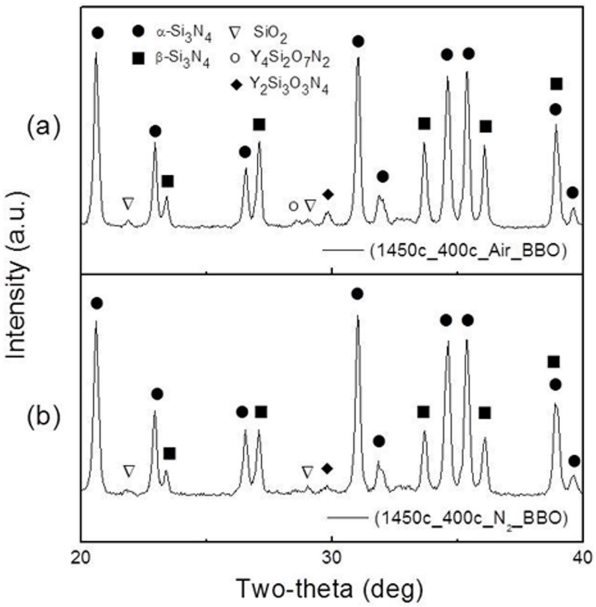

Fig. 2. XRD patterns for Si_3N_4 substrates after nitriding process. Specimens underwent debinding process in (a) air and (b) N_2 atmosphere at 400°C before nitridation at 1450°C (●: α-Si_3N_4 ■: β-Si_3N_4 ▽: SiO_2 o:$Y_4Si_2O_7N_2$ ◆: $Y_2Si_3O_3N_4$).

oxidized Si layer or within Si near the surfaces upon nitridation. When the amount of residual oxygen in the specimen after nitridation was compared with that after debinding, reductions of 2.8% in air and 1.9% in N_2 were observed. Consequently, the following reactions may have occurred:[24-29)]

$$3SiO_2(s) + 2N_2 \rightarrow Si_3N_4(s) + 3O_2 \quad (2)$$
$$Si(s) + SiO_2(s) \rightarrow 2SiO(g) \quad (3)$$

According to the above reactions, degrees of nitridation of ~ 91.2% and ~ 94.2% were obtained when considering Eq. (2) for the specimens debinded in air and N_2 atmospheres, respectively, even when complete nitridation of Si occurred, while degrees of nitridation of ~ 75.9% and ~ 84.1% were calculated in the case of Eq. (3). Therefore, even if nitridation had actually occurred for most of Si, low degrees of nitridation were observed because of the weight reduction.

Figure 3 shows the XRD patterns of Si_3N_4 sintered in different debinding atmospheres. While the α-Si_3N_4 and β-Si_3N_4 crystal phases were present after nitridation, only the high-temperature β-Si_3N_4 phase could be observed in all specimens after sintering, regardless of the debinding atmosphere. As in the case of the XRD patterns obtained after nitriding, although both specimens debinded in air and N_2 showed similar crystal phases, a slightly higher amount of $Y_2Si_3O_3N_4$ secondary phase was observed for the sample debinded in air; this indicated that more secondary phase was formed upon reaction of the larger amount of residual oxygen present in the specimens debinded in air.

Figure 4 shows the surface microstructures of polished and etched Si_3N_4 sintered in different debinding atmospheres. For the polished surface, no pores could be observed, and dense microstructures were present in both specimens debinded in air and N_2 atmospheres. In addition, columnar grains of β-Si_3N_4 as high-temperature phase were observed on the etched surfaces (Fig. 4(c, d)). Although there were no significant differences between the two microstructures, the specimen debinded in air exhibited a relatively larger grain size than the sample debinded in N_2. According to the measured grain size, the columnar grains in the sintered air-debinded specimen had a length of ~ 2 - 4 μm and thickness of ~ 0.7 - 1.2 μm, whereas those in the sintered N_2-debinded specimens had a length of ~2 - 3 μm and thickness of ~ 0.5 - 0.9 μm. Thus, the columnar grains in the sintered air-debinded specimen exhibited relatively larger grain size. As shown in Fig. 2, residual oxygen appeared to play a critical role in the liquid-phase sintering, as the SiO_2 XRD peak present after the nitridation process disappeared after sintering. According to the analysis conducted after nitridation, the oxygen content of the specimen debinded in air, 2.5%, was higher than that of the specimen debinded in N_2, 2.3%. As the viscosity increased with the N/O ratio of the liquid phase, it decreased when the oxygen content increased. This reduction in viscosity enhanced the flowability of the liquid phase; thus, not only a uniform phase transformation occurred throughout the whole specimen, but also the grain growth was affected. Therefore, relatively large amounts of liquid phase in air improve the sinterability, as they increase the grain size.[30)]

Furthermore, the amount of carbon content of specimens debinded in N_2 was 0.2% larger than that of the specimens debinded in air, suggesting the possibility that the resultant generation of SiC obstructed the grain growth.

Figure 5 shows the sintered densities and thermal conductivity values of Si_3N_4 sintered in different debinding

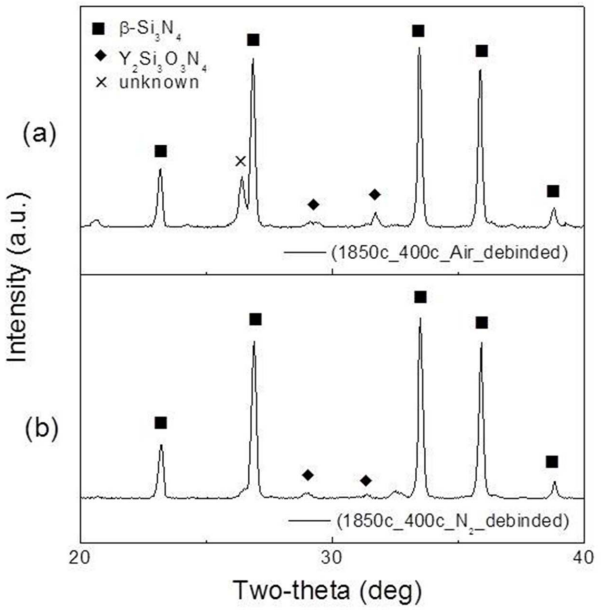

Fig. 3. XRD patterns for Si_3N_4 substrates after sintering at 1850°C for 6 h. Specimens underwent the process of debinding in (a) air and (b) N_2 atmosphere at 400°C before nitridation (■: β-Si_3N_4 ◆: $Y_2Si_3O_3N_4$ x: unknown).

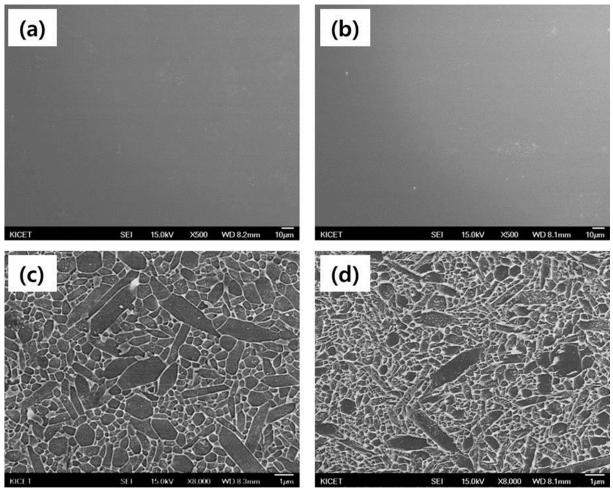

Fig. 4. SEM images for (a, b) polished surface and (c, d) plasma-etched surfaces for Si_3N_4 substrate after sintering at 1850°C for 6 h; (a) and (c) debinded in air, (b) and (d) debinded in N_2 atmosphere.

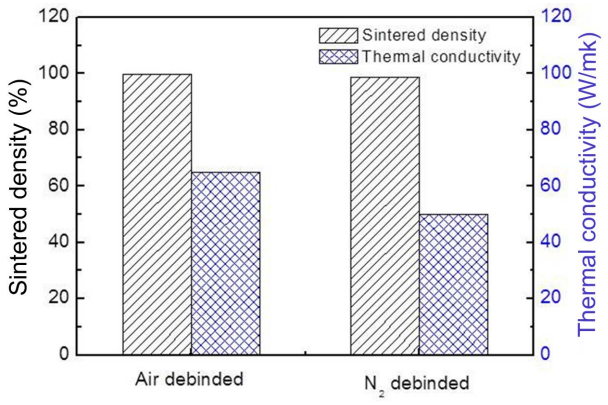

Fig. 5. Sintered density and thermal conductivity for Si_3N_4 substrates debinded in air and N_2 atmosphere after sintering at 1850°C for 6 h.

atmospheres. The relative sintered densities of the specimens debinded in air and N_2 atmospheres were 99.7% and 98.6%, respectively, revealing almost fully densified sintered samples.

The thermal conductivity of the specimen debinded in air was 64.8 W/mK, a value higher than that of the specimen debinded in N_2 (50.1 W/mK). Although thermal conductivities are typically heavily affected by oxygen impurities, the higher thermal conductivity of the Si_3N_4 specimen debinded in air was due to the higher sintered density and larger grain size, as the difference in residual oxygen content between the two specimens was only ~0.2%. [31-33)]

4. Conclusions

In the present study, the effects of the debinding process on the sintered material properties of SRBSN substrates fabricated by the tape casting method were investigated by using different debinding atmospheres. According to the results, only the high-temperature β-Si_3N_4 crystal phase was observed in all specimens after sintering, regardless of the debinding atmosphere, while α-Si_3N_4 and β-Si_3N_4 crystal phases were observed after nitriding. Furthermore, dense microstructures were obtained for samples debinded in both atmospheres, while the Si_3N_4 grain size was relatively larger for specimens debinded in air. The sintered density of the specimens debinded in air was 99.7%, slightly higher than that of the specimens debinded in N_2 (98.6%). The thermal conductivities of the sintered bodies were 64.8 W/mK and 50.1 W/mK for the specimens debinded in air and N_2, respectively; the relatively higher thermal conductivity of the specimen debinded in air was attributed to its higher sintered density and larger grain size.

Acknowledgments

This work was supported by Industrial Technology Innovation Program (No. 10048968) of Korea Evaluation Institute of Industrial Technology (KEIT) grant funded by the Ministry of Trade, Industry and Energy (MOTIE, Korea)

REFERENCES

1. J. S. Lee, J. H. Mun, B. D. Han, D. S. Park, and H. D. Kim, "Effect of Raw-Si Particle Size on the Mechanical Properties of Sintered RBSN," *J. Korean Ceram. Soc.,* **38** [8] 740-48 (2001).
2. M. J. Choi, T. W. Roh, C. Park, D. S. Park, and H. D. Kim, "The Study of Reaction Bonded Silicon Nitride Fabricated Under Static Nitrogen Pressure," *J. Korean Ceram. Soc.,* **37** [5] 505-10 (2000).
3. K. H. Kwak, C. Kim, I. S. Han, and K. S. Lee, "Thermal Shock and Hot Corrosion Resistance of Si_3N_4 Fabricated by Nitrided Pressureless Sintering," *J. Korean Ceram. Soc.,* **46** [5] 478-83 (2009).
4. S. K. Lee, J. D. Morreti, M. J. Readey, and B. R. Lawn, "Thermal Shock Resistance of Silicon Nitrides Using an Indentation-Quench Test," *J. Am. Ceram. Soc.,* **85** [1] 279-81 (2002).
5. B. C. Bae, D. S. Park, W. C. Seo, K. S. Bang, and C. Park, "Microstructural Development of Si_3N_4 Ceramics Containing Aligned β-Si_3N_4 Whisker Seeds," *J. Ocean Eng. Technol.,* **23** [5] 32-8 (2009).
6. K. Hirao, Y. Zhou, H. Hyuga, T. Ohji, and D. Kusano, "High Thermal Conductivity Silicon Nitride Ceramics," *J. Korean Ceram. Soc.,* **49** [4] 380-84 (2012).
7. J. S. Lee, J. H. Mun, B. D. Han, D. S. Park, and H. D. Kim, "Densification Behavior of Reaction-Bonded Silicon Nitride Prepared by Using Coarse Si Powders," *J. Korean Ceram. Soc.*, **39** [1] 45-50 (2002).
8. A. J. Moulson, "Review Reaction-bonded Silicon Nitride: Its Formation and Properties," *J. Mater. Sci.*, **14** [5] 1017-51 (1979).
9. J. R. G. Evans and A. J. Moulson, "The Effect of Impurities on the Densification of Reaction-bonded Silicon Nitride (RBSN)," *J. Mater. Sci.,* **18** [12] 3721-28 (1983).
10. G. Ziegler, J. Heinrich, and G. Wotting, "Review Relationships between Processing, Microstructure and Properties of Dense and Reaction-bonded Silicon Nitride," *J. Mater. Sci.*, **22** [9] 3041-86 (1987).
11. R. G. Pigeon, A. Varma, and A. E. Miller, "Some Factors Influencing the Formation of Reaction-bonded Silicon Nitride," *J. Mater. Sci.,* **28** [7] 1919-36 (1993).
12. Y. Zhou, X. Zhu, and K. Hirao, "Sintered Reaction-bonded Silicon Nitride with High Thermal Conductivity and High Strength," *Int. J. Appl. Ceram. Technol.*, **5** [2] 119-26 (2008).
13. M. N. Rahaman and A. J. Moulson, "The Removal of Surface Silica and its Effect upon Silicon Nitridation Kinetics," *J. Mater. Sci.* **16** [8] 2319-21 (1981).
14. B. Lei, O. Babushkin, and R. Warren, "Nitridation Study of Reaction-bonded Silicon Nitride in situ by High Temperature X-Ray Diffraction," *J. Eur. Ceram. Soc.*, **17** [9] 1113-18 (1997).
15. B. T. Lee, Y. J. Yoon, and K. H. Lee, "Microstructural Characterization of Electroconductive Si_3N_4-TiN Composites," *Mater. Lett.,* **47** [1] 71-6 (2001).
16. J. A. Mangels, "Sintered Reaction Bonded Silicon Nitride,"

Ceram. Eng. Sci. Proc., **2** [7-8] 589-603 (1982).
17. Y. J. Park, M. J. Park, J. M. Kim, J. W. Lee, J. W. Ko, and H. D. Kim, "Sintered Reaction-bonded Silicon Nitrides with High Thermal Conductivity : The Effect of the Starting Si Powder and Si_3N_4 Diluents," *J. Eur. Ceram. Soc.*, **34** [5] 1105-13 (2014).
18. W. G. Yoon, J. J. Kim, and S. H. Cho, "Effects of Particle Size Distribution of Alumina on Behaviors of Tape Casting," *J. Korean Ceram. Soc.*, **34** [11] 1173-81 (1997).
19. J. S. Sung, K. D. Koo, and C. K .Yoon, "Effect of Binder Burnout Temperature on Sintering Shrinkage of Multilayer Ceramics," *J. Korean Ceram. Soc.*, **33** [12] 1373-79 (1996).
20. B. T. Lee, J. H. Yoo, and H. D. Kim, "Fabrication of Silicon Nitride Ceramics Using Semiconductor-Waste-Si Sludge," *Korean J. Mater. Res.*, **9** [12] 1170-75 (1999).
21. B. R. Golla, J. W. Ko, J. M. Kim, and H. D. Kim, "Effect of Particle Size and Oxygen Content of Si on Processing, Microstructure and Thermal Conductivity of Sintered Reaction Bonded Si_3N_4," *J. Alloys Compd.,* **595** 60-6 (2014).
22. W. Y. Park, D. S. Park, H. D. Kim, and B. D. Han, "Sintering and Mechanical Properties of Silicon Nitride Prepared with a Low-cost Silicon Nitride Powder," *J. Korean Ceram. Soc.*, **38** [11] 987-92 (2001).
23. J. S. Park, H. J. Lee, S. S. Ryu, S. M. Lee, H. J. Hwang, and Y. S. Han, "Optimization of Binder Burnout for Reaction Bonded Si_3N_4 Substrate Fabrication by Tape Casting Method," *J. Korean Ceram. Soc.*, **52** [6] 435-40 (2015).
24. S. C. Singhal, "Thermodynamics and Kinetics of Oxidation of Hot-pressed Silicon Nitride," *J. Mater. Sci.,* **11** [3] 500-9 (1976).
25. K. Negita, "Effective Sintering Aids for Si_3N_4 Ceramics," *J. Mater. Sci. Lett.*, **4** [6] 755-58 (1985).
26. M. Liehr, J. E. Lewis, and G. W. Rubloff, "Kinetics of High-temperature Thermal Decomposition of SiO_2 on Si(100)," *J. Vac. Sci. Technol. A*, **5** [4] 1559-62 (1987).
27. F. W. Smith and G. Ghidini, "Reaction of Oxygen with Si(111) and (100): Critical Conditions for the Growth of SiO_2," *J. Electrochem. Soc.*, **129** [6] 1300-6 (1982).
28. D. Starodub, E. P. Gusev, E. Garfunkel, and T. Gustafsson, "Silicon Oxide Decomposition and Desorption during the Thermal Oxidation of Silicon," *Surf. Rev. Lett.,* **6** [1] 45-52 (1999).
29. E. A. Gulbransen and S. A. Jansson, "The High-Temperature Oxidation, Reduction, and Volatilization Reactions of Silicon and Silicon Carbide," *Oxid. Met.,* **4** [3] 181-201 (1972).
30. X. Zhu, Y. Zhou, K. Hirao, T. Ishigaki, and Y. Sakka, "Potential Use of only Yb_2O_3 in Producing Dense Si_3N_4 Ceramics with High Thermal Conductivity by Gas Pressure Sintering," *Sci. Technol. Adv. Mater.*, **11** [6] 1-11 (2010).
31. Y. Zhou, H. Hyuga, D. Kusano, Y. I. Yoshizawa, T. Ohji, and K. Hirao, "Review Article: Development of High-Thermal-Conductivity Silicon Nitride Ceramics," *J. Asian. Ceram. Soc.*, **3** 221-29 (2015).
32. M. Kitayama, K. Hirao, M. Toriyama, and S. Kanzaki, "Thermal Conductivity of β- Si_3N_4: I, Effects of Various Microstructural Factors," *J. Am. Ceram. Soc.*, **82** [11] 3105-12 (1999).
33. X. Zhu, Y. Zhou, and K. Hirao, "Processing and Thermal Conductivity of Sintered Reaction-Bonded Silicon Nitride. I: Effect of Si Powder Characteristics," *J. Am. Ceram. Soc.*, **89** [11] 3331-39 (2006).